Carbon 201 (2023) 659–666

Contents lists available at ScienceDirect

Carbon

journal homepage: www.elsevier.com/locate/carbon

Fluorescent carbon dots synthesis in premixed flames: Influence of the equivalence ratio

C. Russo [a], B. Apicella [a], A. La Rocca [b], M. Sirignano [c,*]

[a] Istituto di Scienze e Tecnologie per l'Energia e la Mobilità Sostenibili, CNR – P.le V. Tecchio, 80 – 80125, Napoli, Italy
[b] Department of Mechanical Materials and Manufacturing Engineering, University of Nottingham, United Kingdom
[c] Univ. Napoli Federico II, Dipartimento di Ingegneria Chimica, dei Materiali e della Produzione Industriale, Napoli, Italy

ARTICLE INFO

Keywords:
Flame synthesis
Carbon dots
Fluorescence
UV–Visible
Quantum yield

ABSTRACT

Flame synthesis could represent a controllable method for production of carbon dots (CDs) with tunable emission properties, alternative to process involving oxidation agents and wet chemistry processing. To control final properties of CDs, a thorough analysis of different reactor parameters has to be conducted. Here we investigate the effect of combustion operative conditions, namely equivalence ratio, for CD production in a premixed flame reactor. CDs with specific optical properties have been synthesized at different equivalence ratios, burning both pure ethylene and ethylene/benzene mixtures. Carbon particulate matter was thermophoretically collected at the exhaust of the flame reactor. Successively, after dichloromethane washing, CDs were simply obtained by N-methyl-pyrrolidone extraction and filtration (<20 nm). In ethylene flames, CDs with fluorescence ranging from green to yellow, as equivalence ratio increases, were synthesized. In ethylene/benzene flames, produced CDs emit fluorescence from blue to green and equivalence ratio seems to play even a more marked role, inducing significant change in the emission spectra with small changes of equivalence ratio. Globally, their quantum yield ranges between 2 and 11%. CDs have been found generally stable for mild change of temperature (up to 80 °C), mild basic pH (pH = 8–10) and over long time at room temperature (up to 240 days). Overall, equivalence ratio demonstrates to be a powerful and simple tool to produce tunable CDs by flame synthesis on large scale.

1. Introduction

Carbon has gained attention as the constituent element for future materials due to its capability to be arranged in different allotropic forms. Fullerenes, nanotubes and graphene nanocarbons opened the challenge of individuating the best way to exploit all their potential. At the same time, research community and industries are seeking for a competitive and effective industrial processes to maximize and making accessible their production on large scale. Among all the carbon nanomaterials arisen in the last years, carbon nanoparticles (CNP), particularly fluorescent CNP - also known as carbon dots (CDs) - have gained great attention due to their features. CDs have showed to be highly biocompatible [1–3] in comparison to semiconductor quantum dots and their intrinsic property of giving photoluminescence [4–6] has made these compounds a promising material for several applications [1–5], including bioimaging, drug delivery and optoelectronics. As stated before, the possibility of effectively use these new nanomaterials is subordinated - among other issues - to finding a way to produce them on large scale, being able to tune their desired features.

Early CD synthesis was mainly based on top-down approach from bulk materials, e.g., laser ablation, electrochemical oxidation and microwave treatment [7]. Bottom-up synthesis approaches [7], based on polymerization and/or carbonization of small molecules to form CDs, have become more and more attractive due to their ease of implementation and tunability.

In this view, flame synthesis has been proposed as source of CDs [8]. Flame reactor is intrinsically autothermic and continuous, making the process suitable for large scale material productions [9–11]. In the past, flame synthesis has been approached to produce fullerenes and nanotubes on large scale [12–17]. Similarly, CNPs ranging from near molecular size up to hundreds of nanometers have been detected in a wide range of combustion conditions [18–22]. However, most of the times, CNPs of different sizes and chemical nature are present simultaneously in the flame at the same location. The role of the sizes in changing the features of CNPs is well known. Hence, one of the possible way to proceed could be collecting all CNPs and separating them on the base of

* Corresponding author.
E-mail address: mariano.sirignano@unina.it (M. Sirignano).

https://doi.org/10.1016/j.carbon.2022.09.061
Received 28 April 2022; Received in revised form 1 September 2022; Accepted 20 September 2022
Available online 26 September 2022

their chemico-physical features, in order to achieve a high grade of purity of the desired CNPs. At same time, it would be possible to optimize the combustion conditions in order to maximize the production of CNPs with desired features. Overall, it is possible to produce CNPs with the same size but differently produced by changing fuel composition, temperature history and equivalence ratio [18–23]. Recently, CD synthesis in controlled flame reactors has been proved to be an effective approach for the direct and easy production of structurally reproducible highly fluorescent CNPs with different emission properties [24]. The fluorescence emission of flame-formed carbons with size <20 nm has shown to be due to a mixture of molecular fluorophores and aromatic domains mainly emitting in the blue region when soluble in dichloromethane (DCM) and to aromatic domains of larger size bonded and/or turbostratically stacked together mainly emitting in the green region when soluble in stronger solvent as N-methyl pyrrolidone (NMP) [24]. Carbon nanostructures with the same properties of CDs – although defined differently - have been historically detected directly in situ by spectral and time-resolved laser induced fluorescence and by other off-line spectroscopic techniques [25–32] by researchers of the combustion community, mainly for inferring their role as intermediates in soot formation. Changing the operative conditions can be used to tune the production of CDs emitting in different wavelength ranges. Recently, we have found that by fueling a premixed flame with mixtures ranging from ethylene to benzene at fixed equivalence ratio, the properties of CDs could be varied and CDs fluorescing from yellow to blue could be easily produced [32].

In this work, the effect of equivalence ratio on the formation of CDs has been explored. In comparison to the previous works [24,32] referring to heavily sooting flames, in the present manuscript we have investigated the equivalence ratio effect in the transition from nearly-to heavily-sooting flames. In particular, both pure ethylene and ethylene/benzene mixture have been fed to a McKenna burner stabilizing a series of premixed flames with different equivalence ratios in order to obtain CDs with specific optical (UV–Visible absorption and fluorescence) properties. Equivalence ratio is one of the simplest process parameters to control and thus the possibility to use it to fine tuning the properties of CDs might open the path for an easily scalable technology for CD flame synthesis on industrial level.

2. Experimental setup

2.1. Flame reactor and configurations

In this work McKenna burner is used to stabilize premixed flames with different fuel mixtures and equivalence ratios (phi), where phi is defined as the ratio of fuel concentration in the actual fuel-air mixture divided by the fuel concentration in a stoichiometric mixture.

In particular, pure ethylene and ethylene/benzene mixture were used to obtain different premixed flames for the CD synthesis. The rule of experiment design is as it follows. Ethylene flames are selected by fixing the cold gas velocity (10 cm/s) and the O_2/N_2 ratio (21/79 – i.e., burning in air). Ethylene flames here investigated have different equivalence ratios (from 2.01 up to 2.46) and they were previously largely analysed both by in situ optical techniques and ex situ analysis of the particle size distribution [26,33–35]. The conditions of the ethylene flames are reported in Table 1. Ethylene/benzene fuel mixtures were also investigated in order to explore the effect of phi in aromatic fuelled flames. Previously, flames with different percentages of benzene in a mixture with ethylene (from 0% to 100%) were studied by keeping constant the equivalence ratio [22,32]. In this work, the ethylene/benzene ratio has been kept constant (50/50 in terms of carbon fed) and the equivalence ratio has been varied from 1.8 up to 2. The choice of having an equivalence ratio lower than in the pure ethylene flame is suggested by the higher propensity of benzene to form particulate of large dimension in flame. In the investigated conditions, the formation of small CDs is hence optimized. Finally, for similarity with pure ethylene flames, in this work ethylene/benzene flames are burned in air (O_2/N_2 ratio equal to 21/79). It is worth to note that, in this setup for CD synthesis, O_2 plays a role of mayor oxidant of species to stabilize the flame and N_2 plays just a diluent role, not entering in CD formation process.

Table 1
Operative conditions of the investigated flames.

	Phi	Cold gas velocity, cm/s	C_2H_4, Mole fraction	O_2, Mole fraction	N_2, Mole fraction	Benzene, Mole fraction
E201	2.01	10	0.1233	0.1841	0.6926	–
E216	2.16	10	0.1313	0.1824	0.6862	–
E231	2.31	10	0.1392	0.1808	0.6800	–
E246	2.46	10	0.1469	0.1792	0.6739	–
EB180	1.80	8	0.0630	0.1924	0.7237	0.0210
EB190	1.90	8	0.0661	0.1915	0.7203	0.0220
EB200	2.00	8	0.0693	0.1906	0.7170	0.0231

All the experimental details on the flames operating conditions are reported in Table 1. Ethylene/benzene flames have been preliminary investigated by optical techniques and particle size distribution in order to assess whether the conditions were suitable for collecting CDs. These preliminary results are not reported here since the focus is on the collected material for which a molecular weight distribution is performed by a chromatographic technique. Future work might systematically investigate these conditions from a different perspective.

2.2. Carbon material sampling and analytical treatment

CD collection and characterization procedures are the same reported in a recent work [32]. Here and in the following subsection a brief description is reported. CD sampling was performed at the end of the flame reactor (HAB = 15 mm) by means of thermophoretic deposition on a glass plate (75 × 25 × 1 mm) horizontally inserted into the flame for a short time (2 s). The insertion procedure was automatized and repeated many times for a total insertion time of 60s. Total insertion time was optimized in order to deposit enough material in form of thin carbon film for the following analysis. This procedure has been tested and validated to avoid experimental artifacts [32,33].

Glass plates covered by carbon material were washed in DCM to remove the light molecular weight (MW) part of the organic carbon. The DCM-insoluble carbon samples were completely removed from the glass plate by dispersion in NMP in an ultrasonic bath (5 min, 59 KHz) and then filtered on an Anotop filter (Whatman) to separate the fraction <20 nm. The fraction <20 nm was analysed by absorption and fluorescence spectroscopy. Fig. 1 reports a sketch of the adopted procedure.

2.3. CD characterization

A HP 8453 Diode Array spectrophotometer was used to perform UV–Visible (UV–Vis) analysis of the carbon samples dissolved in NMP after the filtration. A highly cross-linked individual-pore column (Polymer Laboratories, Ltd, UK) was used to analyse the fraction <20 nm in 100–1E5 u MW range [24,32]. The injection volume was 250 μl and the analyses were performed at a temperature of 80 °C with a flow rate of 0.5 ml/min. The online detection of species eluted from the size exclusion chromatography (SEC) column used a HP1050 UV–Vis diode array detector that measured the absorbance signal at a fixed absorption wavelength (350 nm). The fluorescence measurements were performed on the <20 nm fraction further diluted in NMP to avoid concentration quenching and/or other phenomena. Fluorescence spectra were measured in standard 1 cm path-length quartz cells on HORIBA Scientific FluoroMax-Plus TCSPC spectrofluorometer. It is equipped with a 150 W CW Ozone-free xenon arc lamp, a Czerny-Turner design monochromator with plane gratings for optimized focus at all wavelengths and minimum stray light and an air cooled and stabilized

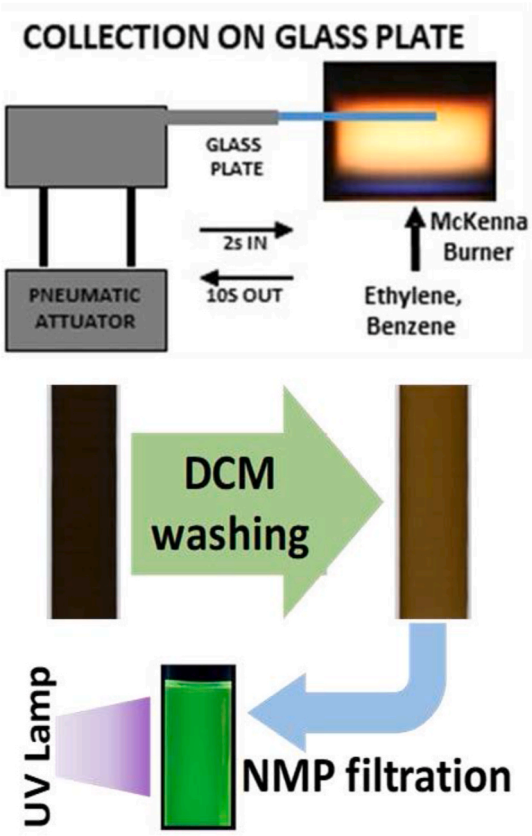

Fig. 1. Schematic representation of sample collection and preparation.

Photomultiplier R928P, operating in a spectral range from 185 to 900 nm. FluoEssence management and analysis software is employed for data acquisition. Quantum yield (QY) of fluorescent species was evaluated at 350 nm by comparison with a standard species (9,10-diphenyl anthracene). The experimental error for SEC, UV–Vis and fluorescence spectroscopy measurements was evaluated to be less than 10%.

For Raman analysis, some drops of CDs in NMP solution were deposited on quartz plates and heated in an oven at 100 °C for few minutes for evaporating the solvent. Raman spectra of the CDs were measured by means of a Horiba XploRA Raman microscope system with an excitation wavelength of $\lambda = 532$ nm (frequency doubled Nd:YAG-solid state laser, 25 mW). The energy on the sample was set at less than 1 mW to avoid sample damage. The Raman spectra were collected with an acquisition time of 30 s and an accumulation of 4 runs. More details are reported in Ref. [36].

TEM analysis was carried out using a JEOL 2100F TEM equipped with a Gatan Orius CCD camera operating at low voltage (40 kV). CDs were dispersed in ethanol by ultrasonic agitation and dropped onto a carbon lacey grid for TEM and HRTEM analysis [37,38]. Several images were acquired in order to make the images statistically significant.

3. Experimental results

3.1. Ethylene flames

Particles were sampled in ethylene/air flames at HAB = 15 mm – i.e., at the end of the flame – on the glass plate following the illustrated procedure. Successively, samples have been washed in DCM in order to eliminate the contribution of DCM-soluble fraction, mainly constituted of C > 20 PAH [39]. These PAHs have shown to be preferentially deposited when the glass plate is rapidly covered by a layer of soot particles, as in fuel-rich conditions. However, in this work, exploring flames with very different sooting tendency by washing the samples in DCM before performing other analysis, we have avoided the sampling-dependent contribution of the low MW fraction of the organic carbon. Once the samples have been dried from DCM, they have been dissolved by sonication in NMP and then filtered to eliminate the fraction with size larger than 20 nm.

In Fig. 2 SEC chromatograms for the CDs, collected in the ethylene flames and isolated following the described procedure, are reported. The figure shows the effectiveness of the procedure in isolating CDs with molecular weight between 10^4 u and $2*10^5$ u – corresponding in spherical and unitary density approximation to 3–8 nm range. CDs in NMP solution have been then spectroscopically analysed to understand their photoluminescence properties. In Fig. 3A UV–Vis spectra normalized at 300 nm of the CDs collected in the four ethylene flames are reported. The features of the spectra measured for CDs collected in flames with different equivalence ratios are significantly different. As the equivalence ratio increases, the visible absorption relatively increases with respect to the UV one, being the CDs collected in the phi = 2.01 flame the most absorbing in the UV.

In Fig. 3B the normalized fluorescence spectra of CDs excited at 350 nm are reported. Following the trend showed for the absorption spectra, the CDs exhibit a shift of the fluorescence emission toward higher wavelengths as the equivalence ratio increases from 2.01 to 2.46. In particular, a significant change between phi = 2.01 and 2.16 can be observed, being the CDs collected in the 2.01 flame mainly blue/cyan emitters (435–530 nm). For the CDs collected in the 2.16 and 2.31 flames the fluorescence spectra are broader with a significant increase of the emission in the green (520–565 nm) and yellow (565–590 nm) wavelength regions accompanied by a gradual decrease of the signals in blue/cyan region as the equivalence ratio increases. The emission spectrum for the CDs collected in the 2.46 flame is sharper and all the fluorescence signal is localized in the green/yellow region. Overall, fluorescence emission shift from blue to green as the equivalence ratio increases can be immediately visually appreciated looking at the photos of the samples reported in Fig. 3C under illumination of a UV lamp@365 nm.

The change of fluorescence spectra can be attributed to a change in the structure. In this case no doping effect due to the presence of heteroatoms can be individuated. In fact, according to the literature on the formation of the first particles, i.e., nucleation process, the internal arrangement of the freshly formed structures depends on the reactor conditions, such as temperature and local equivalence ratio [25,26,40,41]. In the case of premixed flames, the temperature can play a minor role in term of induced differences since particles are always formed in a range of temperature between 1500 and 1700 K [26,40,41]. Differently, in diffusion flames temperature can drop locally around 1000 K,

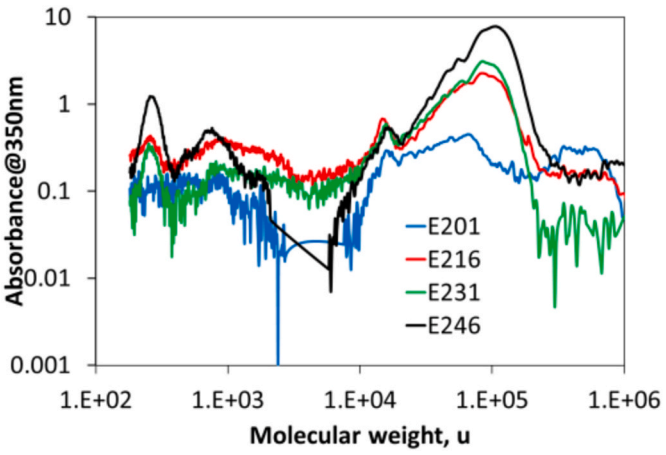

Fig. 2. SEC chromatograms measured at 350 nm of ethylene-formed CDs at different equivalent ratios. (A colour version of this figure can be viewed online.)

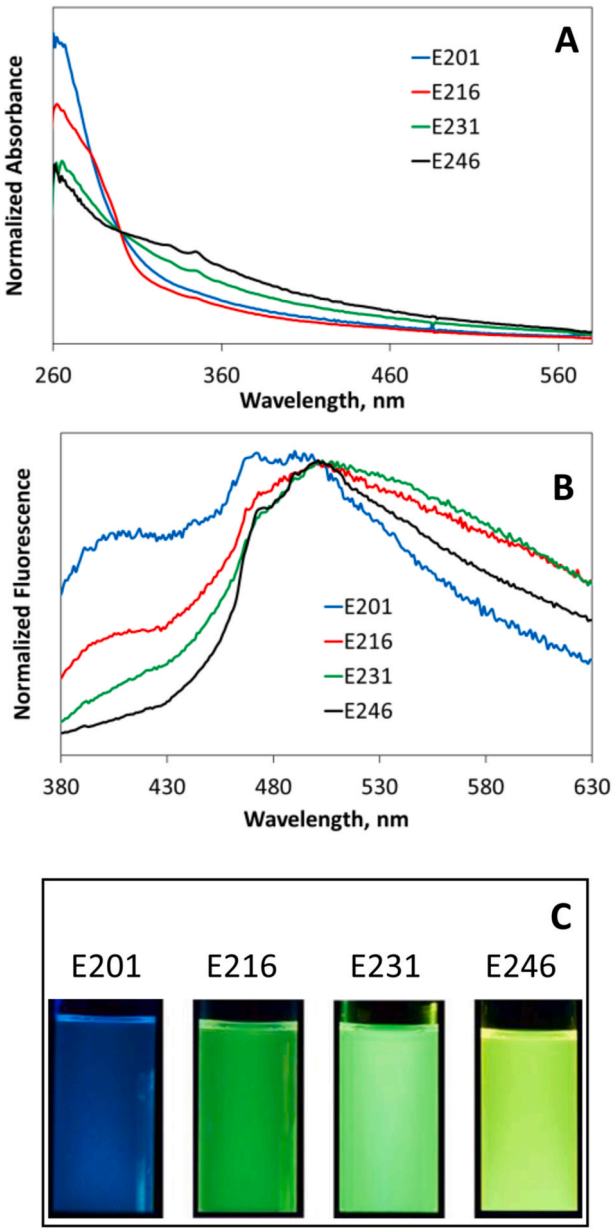

Fig. 3. UV–Vis spectra Normalized at 300 nm (panel A), normalized fluorescence spectra excited at 350 nm (panel B) and photos under illumination of a UV lamp @365 nm (panel C) of ethylene-formed CDs at different equivalent ratios. (A colour version of this figure can be viewed online.)

significantly changing the nucleation process. In premixed condition hence the equivalence ratio determines the effective availability of the large PAHs for nucleation process and formation of these small particles, which can be assimilated to CDs [25,40]. As the equivalence ratio increases, the amount of PAH with larger mean size increases. These latter can be easier arranged in more packed structure. Conversely, at lower equivalence ratio PAHs are smaller in mean size and less abundant. This turns into first structure of CD more loose [25,26,40,42–45]. The different structures both in terms of mean size and internal arrangement have significantly different optical properties. In fact, as the mean size of PAH composing the CDs increases and is arranged in a more packed structure, the interaction between PAHs becomes more significant and it turns into a red shift of the emitted light, as reported in Fig. 3. In the loose structure produced at lower equivalence ratio, the small PAHs are mainly held by crosslinks and this turns into a blue shifted fluorescence [25,26,40,42–45]. Interestingly, the size of these CDs remains confined in a small range of few nanometers. This is due to the fact that, as their size increase exceeding a certain size, they rapidly grow and coagulate to form large particles aggregates. In ethylene flames CDs are continuously freshly generated and thus they can be found at the exhaust of the flames together with large soot aggregates. In general, the examined CDs can be generally described as amorphous. In the yellow fluorescent CDs locally a strong Van der Waal interaction between aromatic planes can be found, however for these CDs globally no lattice structure can be individuated.

By changing the equivalence ratio from 2.01 to 2.16 and then from 2.31 finally to 2.46 implies to move from a non sooting flame to an incipient-sooting flame, to a sooting and to a fully sooting flame, respectively. This means that not only the nucleation process is changing as described, but also the evolution of large soot aggregates significantly changes: large soot aggregates together with small particles – i.e. the CDs are formed in different amount and size [26,33–35]. Overall, as the equivalence ratio increases, the environment conditions for particle formation change less significantly, reaching a sort of saturation effect. In fact, moving beyond 2.46 no further change in the fluorescence spectra was found. This sooting behaviour has been clearly identified in previous works on the same flames [26,33–35]. The CDs seem to be very sensitive to these parameters not only in terms of total amount produced, but also of optical features.

From the UV–Vis and fluorescence spectra it has been possible to estimate the QY reported in Fig. 4 along with the optical band gap [46,47]. According to the model proposed by Robertson and O'Reilly for amorphous carbons [48], the change of the optical band gap for carbon-based material is linked to the change of the length of the aromatic units, namely as the aromatic size increases the band gap decreases. The QY calculated for the flame-formed CDs reported in this paper are similar to those found in our previous works [24,32] and are comparable to those of CDs produced with different synthetic methods [49]. The band gap [46,47] evaluated from the UV–Vis spectra in the 350–700 nm range, slightly increases as the equivalence ratio increases. Although the band gap is related to all the absorbing species, while the QY only to the fluorescing ones, some information can be derived from Fig. 4. The slightly increase of the band gap as the equivalence ratio increases could be attributed to the large presence of high MW absorbing molecules not soluble in DCM. This finding is confirmed by some peaks present in the SEC chromatogram at low MW (Fig. 2) and by the faintly structured absorption around 350 nm (Fig. 3A) characterizing the UV–Vis spectra of CDs collected at 2.31 and 2.46 flames. These species could also contribute to the increase of the QY, being less absorbing having a higher band gap [50]. Interestingly, the QY increases as the equivalence ratio increases and, hence, as the green fluorescence signals increase. The increase of the fluorescence at higher wavelength suggests

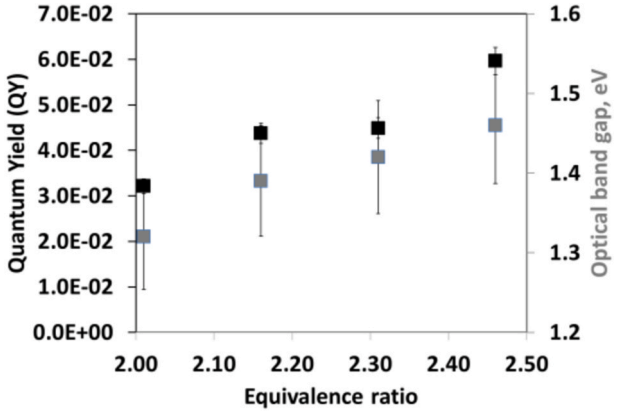

Fig. 4. Quantum yield and optical band gap of ethylene-formed CDs at different equivalent ratios. (A colour version of this figure can be viewed online.)

an increase of the size of the aromatic compounds within the CDs. Alternatively, the formation of CDs with a more stacked structure would explain the red-shift of the fluorescence. These trends suggest that higher equivalence ratio of the flames promotes the growth of the aromatics and the aromatization process of the freshly formed particles in flame. These considerations on the role of aromatic size and stacking have been made also by using laser-induced fluorescence detecting nanoparticles or CDs in flames [25,26].

In order to get more information on the nature of CDs produced in flames with different equivalence ratio, Raman spectra were collected. Raman spectra of CDs present a very intense photoluminescence background and the wings of the bands can easily be confused with the fluorescence background that perturbs also the main Raman peaks, D and G. For this reason, it is not convenient to deconvolve the spectra but to look at them as they are. Raman spectra for CDs collected in the ethylene flames with equivalence ratio of 2.01 and 2.46, representing the extremes of the investigated conditions, are reported in Fig. 5.

I(D)/I(G) ratio are rather similar indicating a similar aromatic layer length extension, while a different broadening of the peaks can be noticed moving from 2.01 to 2.46 equivalence ratio. This is caused by an increased structural disorder due to bond angle and bond length distortions, indicating that clusters probed in the 2.01 sample are more defect-free, unstrained and molecular [51].

A significant shift of the G peak can be also noticed, due to the increase of the sp^3 carbon content and of the bond disorder [52], accordingly with the higher band gap characterizing 2.46 CDs [53]. Overall, Raman measurements confirm the different nature of CDs collected in flames with different equivalence ratio and generally follow the insights gained from previous measurements [45,54].

In order to get more insights on the dimensions, structure and morphology of these CDs, TEM and HRTEM analysis was performed. TEM images of CDs have been acquired by using a voltage much lower than usual (40 keV instead of 200 keV) in order to avoid possible changes induced by the electron beam during measurements. Indeed, when volatile and/or amorphous species are present, to achive a good resolution, it is necessary to use longer exposure times compared to the few seconds typically used for the analysis of soot structure and nanostructure, but this can cause a change in structure and damage the sample [55,56]. The need to apply longer exposure times for CDs synthetized in the present work, achiving a good resolution at all the voltage applied, is indicative of their amorphous character. Therefore, for ruling out the possibility of any beam-induced effect, the CDs images were acquired at a low voltage (40 KeV). A representative image of the CDs collected in ethylene flames with equivalence ratio of 2.46 is reported in Fig. 6, with the scale of 200 nm. A zoom at 20 nm scale is also reported in the inset. According to other measurements on particles produced in this flame reported in this work and previously [26,32,33], this flame condition has to be considered that producing CDs with the most organized structure. It is possible to observe that the typical dimension of the particles is less than 10 nm, in agreement with SEC analysis (Fig. 2). Moreover, the amorphous nature of these small particles is shown in the inset, where the ordered fringes typical of graphitic –like soot are not observable [57]. This helps confirming the amorphous nature of these small CDs.

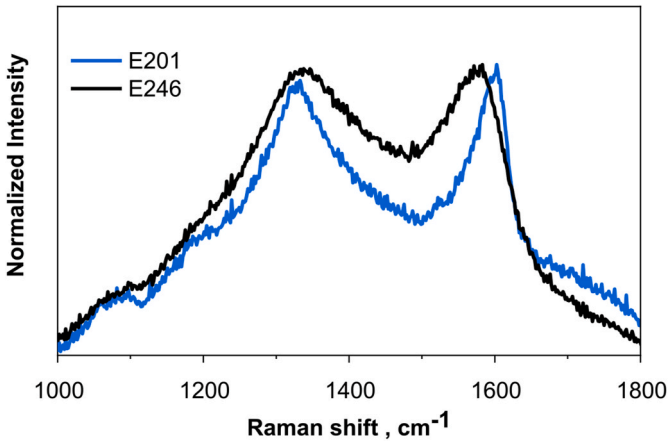

Fig. 5. Normalized Raman spectra for CDs collected in ethylene flames with equivalence ratio of 2.01 and 2.46. (A colour version of this figure can be viewed online.)

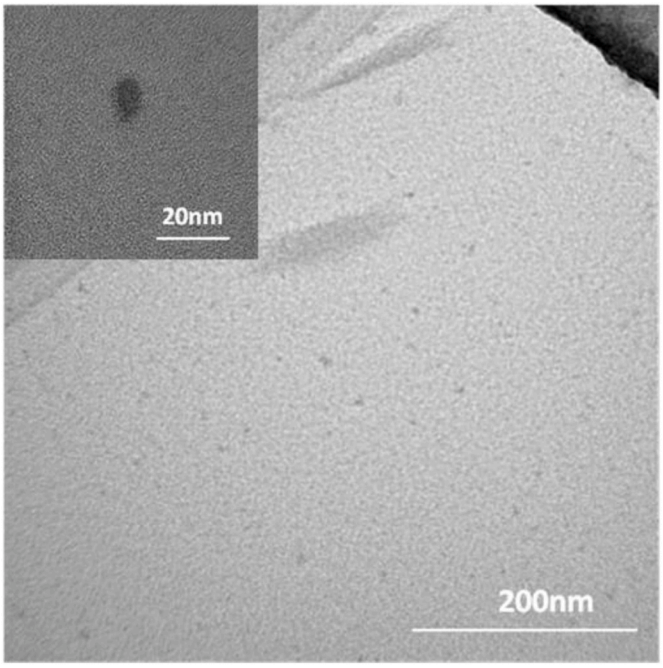

Fig. 6. Representative TEM image for CDs collected in ethylene flames with equivalence ratio of 2.46.

3.2. *Ethylene/benzene flames*

Ethylene/Benzene flames have been analysed in order to investigate whether or not it was possible to tune the fluorescence by changing the equivalence ratio in a flame fuelled with a high percentage of aromatic. The role of aromatic present in the fuel mixture is not trivial. It enhances the formation of PAH since the formation of the first aromatic ring is skipped [22,38,58]. The formation of large amount of PAHs increases the formation of nucleated particles. Due to the fast growth process typical of the aromatic fuelled flames [22,58], CDs mostly end up in forming large soot aggregates and were found in low amount at the exhaust, much lower with respect to the aliphatic flame. As result, at the exhaust the CDs are the remaining ones not ended up in large particles or those slowly formed further on in the flame. The structure of the obtained CDs results similar to the loose ones found in ethylene flames with low equivalence ratio. In fact, from the recent findings [32] it has been demonstrated that CDs exhibiting a blue fluorescence can be obtained in a pure benzene flame. Here we started from an ethylene/benzene mixture with 50% of carbon fed as benzene. Moving from the same equivalence ratio investigated in the past (phi = 2.0), we decided to explore lower equivalence ratios – namely 1.8 and 1.9 – in order to find conditions where the growth towards soot particles was slowed down and CDs were produced in larger amount. Also, by reducing the equivalence ratio, the growth of the aromatic compounds and the aromatization process might also have been slowed down, similarly to what just showed for the ethylene case. As a net result, the CDs produced would have a fluorescence more shifted toward the blue emission region.

The results for the CDs collected in the ethylene/benzene flames are

reported in the panels of Fig. 7. For samples collected in the ethylene benzene flames the absorbance signals in the 350–700 nm range were too low for reliable measurements of the SEC chromatograms and evaluation of optical band gap within a satisfactory tolerance.

However, UV–Vis spectra reported in Fig. 7A are very similar among them and show a quite similar behaviour with the CDs collected from the ethylene flame at the lower equivalence ratio having the largest absorption in the UV region. Looking at the fluorescence spectra with an excitation wavelength of 350 nm reported in Fig. 7B, the changes in the emission as a function of the equivalence ratio appear evident. Fluorescence shift toward higher wavelengths as the equivalence ratio increases is even more evident than for the ethylene case, hence the effect of this parameter for the benzene flames seems quite more important. Also for the ethylene/benzene flame with the highest equivalence ratio investigated (phi = 2.0), CDs show a fluorescence more shifted toward the blue region with respect to those produced in the ethylene flames. In particular, the fluorescence band observed for CDs obtained in ethylene flames peaked at about 520 nm (Fig. 2B) is not present in the CDs collected in the ethylene/benzene flames. As showed in the previous work [32] by fuelling an aromatic molecule, CDs fluorescence is generally shifted towards the blue region. The QY, reported in Fig. 7C, decreases when the equivalence ratio decreases. This feature is similar to the trend found for the pure ethylene flames (Fig. 4). Hence, QY for the flame-formed CDs studied in this work is directly proportional to the equivalence ratio and depends strictly on the chemical structure of the particles. Particles produced at high equivalence ratio are characterized by a more compact structure, which inhibits vibrational movements and leads to stronger fluorescence signals in the visible range at longer wavelengths. On the contrary, the particles formed at low equivalence ratio are smaller and are characterized by a loose structure, which determines easier energy dissipation through roto-vibrational movements [25] and a greater fluorescence in the visible at shorter wavelengths. Overall, the equivalence ratio is able to tune the features of the CDs produced also in the aromatic flames.

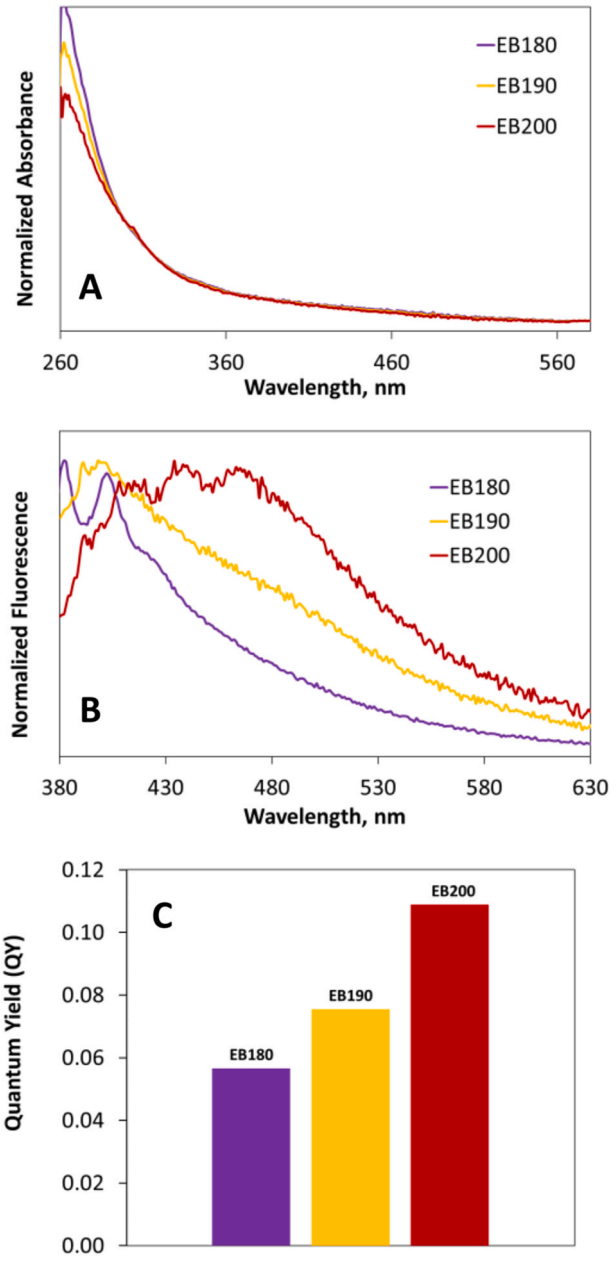

Fig. 7. UV–Vis spectra Normalized at 300 nm (panel A), Normalized Fluorescence spectra excited at 350 nm (panel B) and Quantum Yield at 350 nm of ethylene/benzene-formed CDs at different equivalent ratios. (A colour version of this figure can be viewed online.)

3.3. CD stability over time, temperature and pH

The stability of as prepared CDs vs time, pH and temperature was tested. In Fig. 8, the normalized fluorescence spectra of E246 sample acquired after 1 h, 2 h, 1 and 2 days from the NMP solution preparation were reported. The spectra appeared unchanged over time. Particularly, the fluorescence spectrum acquired after 240 days showed only a small difference of about 4% in the range above 500 nm, as observable in the same figure. Therefore, the CDs appear to be very stable with time also up to hundreds of days.

CD fluorescence stability vs pH was tested in NMP-water solutions in a pH range where the NMP solvent in water has shown to be stable and the spectra obtained have been reported in Fig. 9. Indeed, as reported in Ref. [59], NMP decomposition rate in water solution largely increases with the decrease of pH. The starting pH of pure NMP is basic, about 10 [60], and the progressive addition of water has the effect of decreasing it, moving toward a neutral solution. As observable in Fig. 9, with water addition up to 50% in volume, the fluorescence is constant. In this range of water addition, the estimated pH varies between 8 and 10. Higher percentages of water (66% and more) cause a further decrease of pH and a shift of the fluorescence toward blue region (see also Supplementary Material, Fig. S1). This latter is hence to be most likely ascribed to the NMP decomposition that is known to give this kind of shift, rather than to an instability of CD fluorescence. It is worth to note that the spectra reported are normalized on the maximum intensity. Therefore, in the range of stability of the solvent, CDs showed a significant fluorescence stability over the explored pH range.

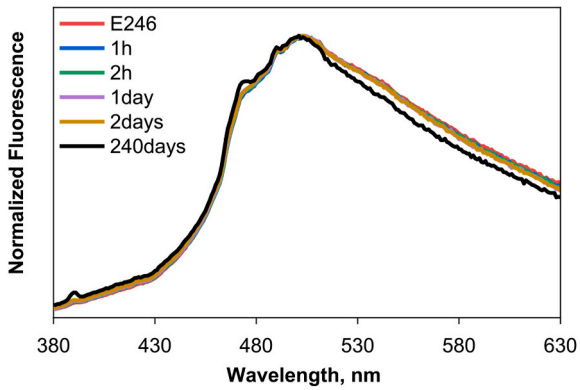

Fig. 8. Height normalized fluorescence spectra, acquired at 350 nm excitation wavelength, of E246 sample vs time. (A colour version of this figure can be viewed online.)

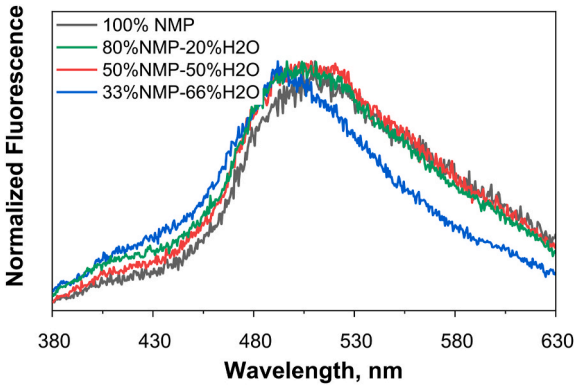

Fig. 9. Height normalized fluorescence spectra, at 350 nm excitation wavelength, of E246 sample vs pH (progressive addition of water to NMP solutions). (A colour version of this figure can be viewed online.)

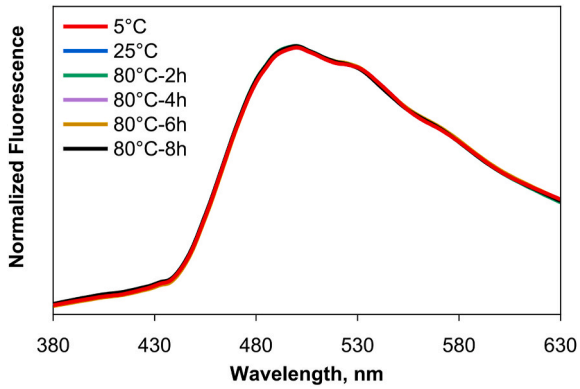

Fig. 10. Normalized fluorescence spectra, at 350 nm excitation wavelength, of E246 sample vs temperature (at 80 °C the acquisition was repeated after temperature exposition of 2, 4,6, 8 h). (A colour version of this figure can be viewed online.)

CD fluorescence stability vs temperature was tested by measuring the fluorescence of E246 at three temperatures: 5, 25 and 80 °C. The highest temperature was chosen in order to avoid NMP degradation and also because it was used in another experiment presented in the paper (see SEC procedure). At the highest temperature (80 °C), the acquisition was also repeated after 2, 4, 6, and 8 h of temperature conditioning. The results are reported in Fig. 10, where it is possible to observe that the spectra acquired at 350 nm of excitation wavelength do not change at all. For the maximum conditioning time and temperature (80 °C for 8 h), NMP was found not significantly degraded and stable in terms of background fluorescence (verified analyzing pure NMP fluorescence spectrum after 8h at 80 °C).

4. Conclusions

Flame reactor in premixed configuration was used to synthesize CDs with tunable fluorescence emissions. Equivalence ratio has been investigated as a key parameter to control combustion and hence CD production . Two different fuel mixtures, namely ethylene and ethylene/benzene, have been used for synthesizing CDs in order to simulate the effect of a pure aliphatic and an aliphatic/aromatic fuel mixture. CDs produced in flames were sampled by means of the thermophoretic deposition on a glass plate, successively washed in DCM in order to remove the DCM-soluble fraction. Once dried, samples were sonicated and dissolved in NMP and finally filtered in order to remove the larger soot particles and the aggregates with sizes larger than 20 nm. The remaining fraction is constituted by CDs of few nanometers, as also confirmed by SEC analysis.

UV–Vis spectra of CDs produced in ethylene flames showed a trend of increasing UV absorption as the equivalence ratio decreases. The fluorescence spectra showed the same trend, with CDs exhibiting a blue-dominated fluorescence for the lowest equivalence ratio, which shifts towards a green/yellow-dominated fluorescence as the equivalence ratio increases. An increased mean size of the constituent PAHs and/or an aromatization/stacking process within the CDs as the equivalence ratio increases is likely responsible for this optical behavior. However, from the Raman, TEM and HRTEM analysis even the CDs produced in the highest equivalence ratio flame show the absence of fringe structure typical of soot particles, exhibiting substantially an amorphous internal organization. These findings are in line with similar considerations made for the nanoparticles detected *in situ* in flame.

CDs produced in ethylene/benzene flames - also for the highest equivalence ratio investigated - exhibit emission signals more shifted towards the blue region with respect to those produced from the pure ethylene flames investigated. Generally, as for the ethylene case, by increasing the equivalence ratio it was possible to move the fluorescence spectra toward the green region.

Finally, CDs have showed to be generally stable for mild change of temperature (up to 80 °C), mild basic pH (pH = 8–10) and over long time at room temperature (up to 240 days).

The use of equivalence ratio, i.e. a powerful and simple tool, to tune the features of the CDs produced with different fuel mixtures opens the possibility of having scalable processes and thus producing CDs by flame synthesis on large scale, making them effectively and largely available for different applications.

CRediT author statement

C. Russo, B. Apicella and M. Sirignano equally contributed to the paper Conceptualization, Methodology, Investigation, and Writing - Original Draft, Review & Editing, A. La Rocca contributed to Methodology and Investigation.

Declaration of competing interest

The authors declare that they have no known competing financial interests or personal relationships that could have appeared to influence the work reported in this paper.

Appendix A. Supplementary data

Supplementary data to this article can be found online at https://doi.org/10.1016/j.carbon.2022.09.061.

References

[1] J. Wang, J. Qiu, A review of carbon dots in biological applications, J. Mater. Sci. 51 (2016) 4728–4738, https://doi.org/10.1007/s10853-016-9797-7. –.
[2] Y. Niu, J. Li, J. Gao, X. Ouyang, L. Cai, Q. Xu, Two-dimensional quantum dots for biological applications, Nano Res. 14 (11) (2021) 3820–3839.
[3] Q. Xu, Y. Niu, J. Li, Z. Yang, J. Gao, L. Ding, .C. Xu, Recent progress of quantum dots for energy storage applications, Carbon Neutrality 1 (1) (2022) 1–18.
[4] S.N. Baker, G.A. Baker, Luminescent carbon nanodots: emergent nanolights, Angew. Chem., Int. Ed. 49 (2010) 6726–6744, https://doi.org/10.1002/anie.200906623.
[5] H. Li, Z. Kang, Y. Liu, S.-T. Lee, Carbon nanodots: synthesis, properties and applications, J. Mater. Chem. 22 (2012) 24230–24253, https://doi.org/10.1039/C2JM34690G.
[6] F. Yan, Z. Sun, H. Zhang, X. Sun, Y. Jiang, Z. Bai, The fluorescence mechanism of carbon dots, and methods for tuning their emission color: a review, Microchim. Acta 186 (2019) 583, https://doi.org/10.1007/s00604-019-3688-y.
[7] Y. Wang, A. Hu, Carbon quantum dots: synthesis, properties and applications, J. Mater. Chem. C 2 (2014) 6921–6939, https://doi.org/10.1039/C4TC00988F. -.
[8] H.P. Liu, T. Ye, C.D. Mao, Fluorescent carbon nanoparticles derived from candle soot, Angew. Chem., Int. Ed. 46 (2007) 6473–6475, https://doi.org/10.1002/ange.200701271.
[9] R. Koirala, S.E. Pratsinis, A. Baiker, Synthesis of catalytic materials in flames: opportunities and challenges, Chem. Soc. Rev. 45 (2016) 3053–3068, https://doi.org/10.1039/C5CS00011D.

[10] R. Strobel, S.E. Pratsinis, Flame aerosol synthesis of smart nanostructured materials, J. Mater. Chem. 17 (2007) 4743–4756, https://doi.org/10.1039/B711652G.
[11] C. Schulz, T. Dreier, M. Fikri, H. Wiggers, Gas-Phase synthesis of functional nanomaterials: challenges to kinetics, diagnostics, and process development, Proc. Combust. Inst. 37 (2019) 83–108, https://doi.org/10.1016/j.proci.2018.06.231.
[12] G.A. Kelesidis, E. Goudeli, S.E. Pratsinis, Flame synthesis of functional nanostructured materials and devices: surface growth and aggregation, Proc. Combust. Inst. 36 (2017) 29–50, https://doi.org/10.1016/j.proci.2016.08.078.
[13] W. Merchan-Merchan, A.V. Saveliev, L. Kennedy, W.C. Jimenez, Combustion synthesis of carbon nanotubes and related nanostructures, Prog. Energy Combust. Sci. 36 (2010) 696–727, https://doi.org/10.1016/j.pecs.2010.02.005.
[14] X. Du, H.Y. Liu, Y.W. Mai, Ultrafast synthesis of multifunctional N-doped graphene foam in an ethanol flame, ACS Nano 10 (2016) 453–462, https://doi.org/10.1021/acsnano.5b05373.
[15] N.K. Memon, S.D. Tse, J.F. Al-Sharab, H. Yamaguchi, A.M.B. Goncalves, B.H. Kear, et al., Flame synthesis of graphene films in open environments, Carbon 49 (2011) 5064–5070, https://doi.org/10.1016/j.carbon.2011.07.024.
[16] Z. Hi, H. Zhu, D. Xie, K. Wang, A. Cao, J. Wei, et al., Flame synthesis of few-layered graphene/graphite films, Chem. Commun. 47 (2011) 3520–3522, https://doi.org/10.1039/C0CC05139J. -.
[17] N.K. Memon, S. D Tse, M. Chhowalla, B.H. Kear, Role of substrate, temperature, and hydrogen on the flame synthesis of graphene films, Proc. Combust. Inst. 34 (2013) 2163–2170, https://doi.org/10.1016/j.proci.2012.06.112.
[18] M. Commodo, G. De Falco, A. Bruno, C. Borriello, P. Minutolo, A. D'Anna, Physicochemical evolution of nascent soot particles in a laminar premixed flame: from nucleation to early growth, Combust. Flame 162 (2015) 3854–3863, https://doi.org/10.1016/j.combustflame.2015.07.022.
[19] B. Zhao, Z. Yang, Z. Li, M.V. Johnston, H. Wang, Particle size distribution function of incipient soot in laminar premixed ethylene flames: effect of flame temperature, Proc. Combust. Inst. 30 (2005) 1441–1448, https://doi.org/10.1016/j.proci.2004.08.104.
[20] M. Thierley, H.H. Grotheer, M. Aigner, Z. Yang, A. Abid, B. Zhao, H. Wang, On existence of nanoparticles below the sooting threshold, Proc. Combust. Inst. 31 (2007) 639–647, https://doi.org/10.1016/j.proci.2006.08.035.
[21] L.A. Sgro, A. De Filippo, G. Lanzuolo, A. D'Alessio, Characterization of nanoparticles of organic carbon (NOC) produced in rich premixed flames by differential mobility analysis, Proc. Combust. Inst. 31 (2007) 631–638, https://doi.org/10.1016/j.proci.2006.08.026.
[22] M. Sirignano, A. Ciajolo, A. D'Anna, C. Russo, Particle formation in premixed ethylene-benzene flames: an experimental and modeling study, Combust. Flame 200 (2019) 23–31, https://doi.org/10.1016/j.combustflame.2018.11.006.
[23] C. Liu, A.V. Singh, C. Saggese, Q. Tang, D. Chen, K. Wan, M. Vinciguerra, M. Commodo, G. De Falco, P. Minutolo, A. D'Anna, H. Wang, Flame-formed carbon nanoparticles exhibit quantum dot behaviors, Proc. Natl. Acad. Sci. USA 116 (2019) 12692–12697, https://doi.org/10.1073/pnas.1900205116.
[24] C. Russo, B. Apicella, A. Ciajolo, Blue and green luminescent carbon nanodots from controllable fuel-rich flame reactors, Sci. Rep. 9 (2019), 14566 https://doi.org/s41598-019-50919-1.
[25] M. Sirignano, A. Collina, M. Commodo, P. Minutolo, A. D'Anna, Detection of aromatic hydrocarbons and incipient particles in an opposed-flow flame of ethylene by spectral and time-resolved laser induced emission spectroscopy, Combust. Flame 159 (2012) 1663–1669, https://doi.org/10.1016/j.combustflame.2011.11.005. -.
[26] M. Sirignano, D. Bartos, M. Conturso, M. Dunn, A. D'Anna, A.R. Masri, Detection of nanostructures and soot in laminar premixed flames, Combust. Flame 176 (2017) 299–308, https://doi.org/10.1016/j.combustflame.2016.10.009.
[27] S. Bejaoui, X. Mercier, P. Desgroux, E. Therssen, Laser induced fluorescence spectroscopy of aromatic species produced in atmospheric sooting flames using UV and visible excitation wavelengths, Combust. Flame 161 (2014) 2479–2491, https://doi.org/10.1016/j.combustflame.2014.03.014. -.
[28] A. Bruno, M. Alfè, B. Apicella, C. de Lisio, P. Minutolo, Characterization of nanometric carbon materials by time-resolved fluorescence polarization anisotropy, Opt Laser. Eng. 44 (2006) 732–746, https://doi.org/10.1016/j.optlaseng.2005.03.013.
[29] A. Ciajolo, R. Ragucci, B. Apicella, R. Barbella, M. de Joannon, A. Tregrossi, Fluorescence spectroscopy of aromatic species produced in rich premixed ethylene flames, Chemosphere 42 (2001) 835–841, https://doi.org/10.1016/S0045-6535(00)00258-7.
[30] B. Apicella, R. Barbella, A. Ciajolo, A. Tregrossi, Comparative analysis of the structure of carbon materials relevant in combustion, Chemosphere 51 (2003) 1063–1069, https://doi.org/10.1016/S0045-6535(02)00715-4.
[31] X. Mercier, O. Carrivain, C. Irimiea, A. Faccinetto, E. Therssen, Dimers of polycyclic aromatic hydrocarbons: the missing pieces in the soot formation process, Phys. Chem. Chem. Phys. 21 (2019) 8285–8294, https://doi.org/10.1039/C9CP00394K.
[32] M. Sirignano, C. Russo, A. Ciajolo, One-step synthesis of carbon nanoparticles and yellow to blue fluorescent nanocarbons in flame reactors, Carbon 156 (2020) 370–377, https://doi.org/10.1016/j.carbon.2019.09.068.
[33] C. Russo, A. D'Anna, A. Ciajolo, M. Sirignano, The effect of butanol isomers on the formation of carbon particulate matter in fuel-rich premixed ethylene flames, Combust. Flame 199 (2019) 122–130, https://doi.org/10.1016/j.combustflame.2018.10.025.
[34] M. Salamanca, M. Sirignano, A. D'Anna, Particulate formation in premixed and counter-flow diffusion ethylene/ethanol flames, Energy Fuel. 26 (2012) 6144–6152, https://doi.org/10.1021/ef301081q. -.
[35] M. Conturso, M. Sirignano, A. D'Anna, Effect of 2, 5-dimethylfuran doping on particle size distributions measured in premixed ethylene/air flames, Proc. Combust. Inst. 36 (2017) 985–992, https://doi.org/10.1016/j.proci.2016.06.048.
[36] C. Russo, A. Ciajolo, Effect of the flame environment on soot nanostructure inferred by Raman spectroscopy at different excitation wavelengths, Combust. Flame 162 (6) (2015) 2431–2441.
[37] C. Russo, A. Ciajolo, S. Cimino, V. La Matta, A. La Rocca, B. Apicella, Reactivity of soot emitted from different hydrocarbon fuels: effect of nanostructure on oxidation kinetics, Fuel Process. Technol. 236 (2022), 107401.
[38] S.A. Pfau, A. La Rocca, E. Haffner-Staton, G.A. Rance, M.W. Fay, R.J. Brough, S. Malizia, Comparative nanostructure analysis of gasoline turbocharged direct injection and diesel soot-in-oil with carbon black, Carbon 139 (2018) 342–352.
[39] C. Russo, B. Apicella, A. Tregrossi, M.M. Oliano, A. Ciajolo, Thermophoretic sampling of large PAH (C ≥ 22–24) formed in flames, Fuel 263 (2020), 116722, https://doi.org/10.1016/j.fuel.2019.116722.
[40] A. D'Anna, Combustion-formed nanoparticles, Proc. Combust. Inst. 32 (1) (2009) 593–613.
[41] H. Wang, Formation of nascent soot and other condensed-phase materials in flames, Proc. Combust. Inst. 33 (1) (2011) 41–67.
[42] M. Commodo, G. De Falco, A. Bruno, C. Borriello, P. Minutolo, A. D'Anna, Physicochemical evolution of nascent soot particles in a laminar premixed flame: from nucleation to early growth, Combust. Flame 162 (10) (2015) 3854–3863.
[43] F. Ossler, T. Metz, M. Aldén, Picosecond laser-induced fluorescence from gas-phase polycyclic aromatic hydrocarbons at elevated temperatures. I. Cell measurements, Appl. Phys. B 72 (4) (2001) 465–478.
[44] F. Ossler, T. Metz, M. Aldén, Picosecond laser-induced fluorescence from gas-phase polycyclic aromatic hydrocarbons at elevated temperatures. II. Flame-seeding measurements, Appl. Phys. B 72 (4) (2001) 479–489.
[45] G. De Falco, M. Commodo, P. Minutolo, A. D'Anna, Flame-formed carbon nanoparticles: morphology, interaction forces, and Hamaker constant from AFM, Aerosol. Sci. Technol. 49 (5) (2015) 281–289.
[46] J. Tauc, R. Grigorovici, A. Vancu, Optical properties and electronic structure of amorphous germanium, Phys. Status Solidi 15 (1966) 627–637, https://doi.org/10.1002/pssb.19660150224. -.
[47] C. Russo, B. Apicella, A. Tregrossi, A. Ciajolo, K. Cuong Le, S. Török, P.-E. Bengtsson, Optical band gap analysis of soot and organic carbon in premixed ethylene flames: comparison of in-situ and ex-situ absorption measurements, Carbon 158 (2020) 89–96, https://doi.org/10.1016/j.carbon.2019.11.087.
[48] J. Robertson, E.P. O'Reilly, Electronic and atomic structure of amorphous carbon, Phys. Rev. 35 (1987) 2946–2957, https://doi.org/10.1103/PhysRevB.35.2946.
[49] P. Zuo, X. Lu, Z. Sun, Y. Guo, H. He, A review on syntheses, properties, characterization and bioanalytical applications of fluorescent carbon dots, Microchim. Acta 183 (2016) 519–542, https://doi.org/10.1007/s00604-015-1705-3.
[50] C. Russo, F. Stanzione, A. Ciajolo, A. Tregrossi, Study on the contribution of different molecular weight species to the absorption UV–Visible spectra of flame-formed carbon species, Proc. Combust. Inst. 34 (2013) 3661–3668, https://doi.org/10.1016/j.proci.2012.06.097. -.
[51] C.F.A.R.J. Casiraghi, A.C. Ferrari, J. Robertson, Raman spectroscopy of hydrogenated amorphous carbons, Phys. Rev. B 72 (8) (2005), 085401.
[52] A.C. Ferrari, J. Robertson, Interpretation of Raman spectra of disordered and amorphous carbon, Phys. Rev. B 61 (20) (2000), 14095.
[53] A. Menon, J.A. Dreyer, J.W. Martin, J. Akroyd, J. Robertson, M. Kraft, Optical band gap of cross-linked, curved, and radical polyaromatic hydrocarbons, Phys. Chem. Chem. Phys. 21 (29) (2019) 16240–16251.
[54] G. Rusciano, A.C. De Luca, A. D'Alessio, P. Minutolo, G. Pesce, A. Sasso, Surface-enhanced Raman scattering study of nano-sized organic carbon particles produced in combustion processes, Carbon 46 (2) (2008) 335–341.
[55] D. Ugarte, Curling and closure of graphitic networks under electron-beam irradiation, Nature 359 (6397) (1992) 707–709.
[56] B. Apicella, P. Pre, J.N. Rouzaud, J. Abrahamson, R.L. Vander Wal, A. Ciajolo A, A. Tregrossi, C. Russo, Laser-induced structural modifications of differently aged soot investigated by HRTEM, Combust. Flame 204 (2019) 13–22.
[57] B. Apicella, P. Pre, M. Alfè, A. Ciajolo, V. Gargiulo, C. Russo, A. Tregrossi, D. Deldique, N.J. Rouzaud, Soot nanostructure evolution in premixed flames by high resolution electron transmission microscopy (HRTEM), Proc. Combust. Inst. 35 (2) (2015) 1895–1902.
[58] M. Sirignano, M. Alfè, A. Tregrossi, A. Ciajolo, A. D'Anna, Experimental and modeling study on the molecular weight distribution and properties of carbon particles in premixed sooting flames, Proc. Combust. Inst. 33 (1) (2011) 633–640.
[59] M. Aliabadi, H. Ghahremani, F. Izadkhah, T. Sagharigar, Photocatalytic degradation of N-methyl-2-pyrrolidone in aqueous solutions using light sources of UVA, UVC and UVLED, Fresenius Environ. Bull. 21 (8) (2012) 2120–2125.
[60] G. Lennon, S. Willox, R. Ramdas, S.J. Funston, M. Klun, R. Pieh, .D.F. Cobice, Assessing the oxidative degradation of N-methylpyrrolidone (NMP) in microelectronic fabrication processes by using a multiplatform analytical approach, J. Anal. Methods Chem. (2020).